Dependence of microelastic-plastic nonlinearity of martensitic stainless steel on fatigue damage accumulation

John H. Cantrell

NASA Langley Research Center

Mail Stop 231

Hampton, VA 23681 USA

(Received

Self-organized substructural arrangements of dislocations formed in wavy slip metals during cyclic stress-induced fatigue produce substantial changes in the material microelastic-plastic nonlinearity, a quantitative measure of which is the nonlinearity parameter β extracted from acoustic harmonic generation measurements. The contributions to β from the substructural evolution of dislocations and crack growth for fatigued martensitic 410Cb stainless steel are calculated from the Cantrell model [Proc. Roy. Soc. London A **460**, 757 (2004)] as a function of percent full fatigue life to fracture. A wave interaction factor f_{WI} is introduced into the model to account experimentally for the relative volume of material fatigue damage included in the volume of material swept out by an interrogating acoustic wave. For cyclic stress-controlled loading at 551 MPa and $f_{WI} = 0.013$ the model predicts a monotonic increase in β from dislocation substructures of almost 100 percent from the virgin state to roughly 95 percent full life. Negligible contributions from cracks are predicted in this range of fatigue life. However,

over the last five percent of fatigue life the model predicts a rapid monotonic increase of β by several thousand percent that is dominated by crack growth. The theoretical predictions are in good agreement with experimental measurements of 410Cb stainless steel samples fatigued in uniaxial, stress-controlled cyclic loading at 551 MPa from zero to full tensile load with a measured f_{WI} of 0.013.

PACS numbers: 62.20.Mk; 61.72.Hh; 62.65.+k; 43.25.Ba

I. INTRODUCTION

Cantrell[1] has shown that self-organized substructural arrangements of dislocations formed in wavy slip metals during cyclic stress-induced fatigue produce substantial changes in the microelastic-plastic nonlinearity of the material that is quantified by a material nonlinearity parameter β. The β parameter can be determined directly from acoustic harmonic generation measurements[2,3]. For a given state of fatigue β is highly dependent on the volume fractions of veins and persistent slip bands (PSBs), PSB internal stresses, dislocation loop lengths, dipole heights, and the densities of secondary dislocations in the substructures. More recently, the contribution to β from crack growth has been obtained[4] by applying the Paris-Erdogan[5] equation for crack propagation to the Nazarov-Sutin[6] crack nonlinearity equation. The resulting expression is combined with the Cantrell[1] substructural nonlinearity model to assess the value of β at each stage of the fatigue process from the virgin state to fracture.

Application of the model to stress-controlled cyclic loading of polycrystalline nickel as a function of percent total fatigue life from the virgin state to fracture predicts that for cyclic stress-controlled loading conditions at 241 MPa and at 345 MPa the values of the nonlinearity parameters above 0.01 percent total life differ by no more than three percent despite large differences in the characteristic values of the fatigue-generated substructures[4]. The close agreement for such disparate loads may mean that the manner in which the dislocation substructures evolve during fatigue influences the value of β at a given fatigue state more than the specific values of the dislocation densities and volume fractions of the substructures involved. Although the Cantrell model was developed for cyclic fatigue in metals having a wavy dislocation slip character, fundamental to the

analytical development are the contributions of dislocation monopoles and dipoles as building blocks for the generated fatigue substructures. The dependence on fundamental dislocation arrangements and the relative insensitivity to the specific values of the substructural parameters suggest that the model may be somewhat more generic than originally considered. Thus, the model may be applicable to a variety of materials, perhaps even planar dislocation slip materials, for calculating the fatigue dependence of β by accounting appropriately for differences in the fundamental material parameters, providing that the substructural evolution in the material occurs in a manner that is organizationally and temporally (in terms of percent full life) similar to that of polycrystalline nickel.

It is important to note that experimental measurements using acoustic harmonic generation techniques may involve wave propagation volumes (wave-front cross-sectional area times wave propagation distance) larger than that of the material containing the relevant fatigue-generated substructures (damage). The value of the nonlinearity parameter measured in such cases would be smaller than the value that is properly representative of the extent of fatigue damage. To account for this disparity a wave interaction factor, defined as the ratio of the material damage volume encountered by the wave to the total propagation volume swept out by the wave, is introduced into the model. It is essential that the wave interaction factor be accounted in the measurement process.

In Sect. II a summary of the salient features of the Cantrell model is presented and a method to determine experimentally the wave interaction factor is introduced. The model is applied in Sect. III to a calculation of β versus percent total fatigue life for

martensitic 410Cb stainless steel. The results of the calculations are compared to experimental measurements.

II. SALIENT FEATURES OF THE MODEL AND METHOD FOR DETERMINING THE WAVE INTERACTION FACTOR

A. Fatigue-generated substructures and microelastic-plastic nonlinearity

Nonlinear acoustical experiments[7-10] indicate that metal fatigue may be characterized by a unique nonlinear relationship between an impressed stress perturbation (e.g., a sound wave) and a microelastic-plastic straining of the material at each stage of the fatigue process from the virgin to fracture. The straining is quantified by an experimentally determined material (acoustic) nonlinearity parameter β that increases monotonically by several hundred percent over the fatigue life. In wavy slip materials during fatigue, the initial cycles of alternating stress generate dislocation monopoles that accumulate on the primary glide planes of the material in the form of mutually trapped primary dislocation dipoles. Continued cycling results in the growth of a vein structure formed from the accumulation of dipoles[11]. The process of mutual trapping and accumulation of dislocations continues until the vein structure is composed almost entirely of dislocation dipoles.

The growth of vein structure continues until a critical value of dislocation density is attained that results in a substructural elastic instability[12]. The instability leads to the transformation of some of the vein structure to a more stable persistent slip band (PSB) structure[13.14]. The PSB structure consists of ladder-like arrays of densely-packed dislocation dipoles but with continued cyclic loading the PSBs eventually evolve into a

more cellular structure as the old PSBs harden and new PSBs with the ladder structure are initiated.

Crack nucleation occurs primarily at the intersection of a PSB with a bounding surface that gives rise to a stress singularity[14]. The density of microcracks nucleated during the first 20-40 percent of fatigue life is substantial, but the cracks do not contribute significantly to the material nonlinearity until the crack length reaches a critical value. This critical value does not typically occur for high cycle fatigue of most metals until roughly 80 – 90 percent of the fatigue life is expended. The plastic zone around the crack tip is comprised of the same dislocation substructures (veins, PSBs, cell structures, etc.) that occur in single crystal material cyclically loaded in plastic strain control[15], except that the substructures are more highly localized.

Thus, both dislocation monopoles and dipoles contribute to the nonlinearity parameter of the material. The contribution from monopoles is obtained as[1]

$$\beta^{mp} = \frac{24}{5} \frac{\Omega \Lambda^{mp} L^4 R^3 \left(A_2^e\right)^2}{G^3 b^2} |\sigma_0| \qquad (1)$$

where G is the shear elastic modulus, b is the amplitude of the Burgers vector, and $|\sigma_0|$ is the magnitude of the initial (residual or internal) longitudinal stress in the material, Λ^{mp} is the density of isolated single dislocations (dislocation monopoles) lying in arbitrary slip planes in the grains of polycrystalline solids, R is the Schmid or resolving factor from longitudinal to shear wave propagation, Ω is the conversion factor from shear to

longitudinal strain, L is the average dislocation half-loop length, and A_2^e is the second order Huang coefficient of the polycrystalline material.

The contribution from dislocation dipoles to the nonlinearity parameter is[1]

$$\beta^{dp} = \frac{16\pi^2 \Omega R^2 \Lambda^{dp} h^3 (1-\nu)^2 (A_2^e)^2}{G^2 b} \tag{2}$$

where ν is Poisson's ratio, h is the dipole height (distance between parallel slip directions of a dislocation dipole), and Λ^{dp} is the dislocation dipole density. In addition to the contributions from dislocation monopoles and dipoles the contribution to the material nonlinearity parameter from elastic anharmonicity is[1]

$$\beta^e = -\frac{A_3^e}{A_2^e} \quad . \tag{3}$$

where A_3^e is the third-order Huang coefficient.

Cantrell[1] found from a consideration of the interactions of the stress and strain fields associated with the dislocation monopole, dislocation dipole, and elastic contributions that the effective nonlinearity parameter β is not a simple sum of the individual contributions given in Eqs. (1)-(3), but rather is given by

$$\beta = \frac{\beta^e + \beta^{mp} + \beta^{dp}}{\left(1 + \Gamma^{mp} + \Gamma^{dp}\right)^2} \tag{4}$$

where the gamma factors

$$\Gamma^{mp} = \frac{2}{3}\left(\frac{\Omega\Lambda^{mp}L^2R}{G}\right)A_2^e \tag{5}$$

and

$$\Gamma^{dp} = \frac{4\pi A_2^e \Omega R \Lambda^{dp} h^2 (1-\nu)}{G} \ . \tag{6}$$

Equation (4) is obtained under the assumption that the dislocation monopoles and dipoles are distributed uniformly throughout the material. For wavy slip metals, the monopoles and dipoles are not distributed uniformly but are confined mostly to the discrete vein and PSB substructures generated in the material during fatigue. We denote the total volume fraction of substructure containing monopoles by f^{mp} and the total volume fraction of substructure containing dipoles by f^{dp}. We assume that the values of the monopole and dipole nonlinearity parameters, β^{mp} and β^{dp}, and gamma factors, Γ^{mp} and Γ^{dp}, are constant within the fatigue-generated substructures.

The dislocation dipole contribution has a possible vein structure source and a possible PSB source depending on the state of fatigue. We thus write $f^{dp}\beta^{dp} = f_{vein}\beta_{vein}^{dp} + f_{PSBw}\beta_{PSBw}^{dp}$ and $f^{dp}\Gamma^{dp} = f_{vein}\Gamma_{vein}^{dp} + f_{PSBw}\Gamma_{PSBw}^{dp}$ where f_{vein} and f_{PSBw}, respectively, are the volume fractions of material at a given percent full life containing vein structure and PSB wall structure. The dislocation monopole contribution has a vein structure source and a PSB structure source resulting from the generation of secondary dislocations in the PSBs as they mature. Hence, we write $f^{mp}\beta^{mp} = f_{vein}\beta_{vein}^{mp} + f_{PSB\sigma}\beta_{PSB\sigma}^{mp}$ and $f^{mp}\Gamma^{mp} = f_{vein}\Gamma_{vein}^{mp} + f_{PSB\sigma}\Gamma_{PSB\sigma}^{mp}$ where $f_{PSB\sigma}$ is the volume

fraction of material within the PSBs that contains sufficiently large secondary dislocation densities to significantly influence β via the PSB internal stress field. From a consideration of the organizational detail of the dislocation substructures that evolve during the fatigue process we obtain that the effective nonlinearity parameter for wavy slip metals is more appropriately given as[1,4]

$$\beta = \frac{\beta^{e} + f_{vein}\left(\beta_{vein}^{mp} + \beta_{vein}^{dp}\right) + f_{PSB}\left(0.15\beta_{PSB\sigma}^{mp} + 0.125\beta_{PSBw}^{dp}\right)}{\left[1 + f_{vein}\left(\Gamma_{vein}^{mp} + \Gamma_{vein}^{dp}\right) + f_{PSB}\left(0.15\Gamma_{PSB\sigma}^{mp} + 0.125\Gamma_{PSBw}^{dp}\right)\right]^{2}} . \qquad (7)$$

B. The effects of fatigue crack growth

In order to determine the crack contribution to the total nonlinearity parameter as a function of crack growth during the fatigue process, Cantrell[4] applied the Paris-Erdogan[5] equation to the Nazarov-Sutin[6] crack nonlinearity equation. He derived that the crack contribution β^{crk} at given fraction of total fatigue life f measured from the virgin state is obtained as

$$\beta^{crk} = \frac{5.3x10^{6} C_{crk}}{\left[a_1^{n-2} + a_2(1-f)\right]^{8/(n-2)}}\left[1 + \frac{0.25C_{crk}}{\left[a_1^{n-2} + a_2(1-f)\right]^{6/(n-2)}}\right]^{-2} \qquad (8)$$

where

$$a_1 = \frac{B\sigma_{\max}}{K_{1c}} \qquad (9)$$

and

$$a_2 = \frac{(n-2)}{2} N_{total} A(B\Delta\sigma)^n \qquad (10)$$

C_{crk} is the crack concentration; $\Delta\sigma$ is the applied stress range (maximum stress minus minimum stress) during cyclic loading; N_{total} is the total number of fatigue cycles from the virgin state to fracture; K_{1c} is the fracture toughness of the material; B is a factor that depends on the geometry of the crack ($\approx$ 1.13 for penny-shaped cracks); and A and n are material-dependent constants experimentally determined for a given material.

It is emphasized that Eq.(8) applies in the Paris law regime where the crack radius is of the order 250 μm or larger. Such crack lengths generally occur in the final 10-20 percent of fatigue life for high cycle fatigue. Cracks having a radius smaller than 250 μm make a negligible contribution to β^{crk} for typical values of C_{crk} (of order[6] $10^7 m^{-3}$).

C. The wave interaction factor

As mentioned previously, ultrasonic measurements may involve wave propagation volumes larger than that of the material encountered by the wave containing relevant fatigue damage. The value of the nonlinearity parameter measured in such cases will always be smaller than the value that is properly representative of the fatigue damage. In order to correct for this disparity we define the ratio of the damage volume encountered by the wave to the total wave propagation volume to be the wave interaction factor f_{WI}. The equation for the effective nonlinearity parameter is then more appropriately written in terms of the wave interaction factor as

$$\beta = \frac{\beta^e + f_{WI} f_{vein}\left(\beta_{vein}^{mp} + \beta_{vein}^{dp}\right) + f_{WI} f_{PSB}\left(0.15\beta_{PSB\sigma}^{mp} + 0.125\beta_{PSBw}^{dp}\right)}{\left[1 + f_{WI} f_{vein}\left(\Gamma_{vein}^{mp} + \Gamma_{vein}^{dp}\right) + f_{WI} f_{PSB}\left(0.15\Gamma_{PSB\sigma}^{mp} + 0.125\Gamma_{PSBw}^{dp}\right)\right]^2} \quad . \qquad (11)$$

Note that the wave interaction factor includes contributions to β both from veins and PSBs. The individual contributions to β from veins and PSBs are accounted by the factors f_{vein} and f_{PSB}. Although variations in f_{vein} and f_{PSB} most certainly occur in different regions of fatigue damage, such detailed information is generally not available for any material and we are limited to the approximations assumed here.

In order to assess the value of f_{WI} we turn to the equation obtained by Cantrell[1] for the effective second order Huang elastic constants of fatigued material $(A_2^e)_{effect}$ (= Q^{-1} in Ref. 1). We modify the equation to account for the wave interaction factor f_{WI}, by writing

$$\left(A_2^e\right)_{effect} = \frac{A_2^e}{\left[1 + f_{WI} f_{vein}\left(\Gamma_{vein}^{mp} + \Gamma_{vein}^{dp}\right) + f_{WI} f_{PSB}\left(0.15\Gamma_{PSB\sigma}^{mp} + 0.125\Gamma_{PSBw}^{dp}\right)\right]} \qquad (12)$$

where A_2^e is the second order Huang constant in the virgin state. The effective second order Huang constant is obtained directly from ultrasonic phase velocity measurements as $(A_2^e)_{effect} = \rho_0 v^2$, where v is the phase velocity and ρ_0 is the mass density of the material. Hence, measurements of the mass density and the ultrasonic phase velocities in the virgin state and fatigue state, respectively, will yield A_2^e and $(A_2^e)_{effect}$. The wave interaction factor f_{WI} can then be determined from Eq.(12).

III. APPLICATION OF MODEL TO MARTENSITIC 410Cb STAINLESS STEEL

A. General considerations

We consider the application of the above model to the calculation of the nonlinearity parameters of martensitic 410Cb stainless steel as a function of percent full fatigue life to fracture. Grobstein *et al.*[16] published an extensive study of substructural evolution in fatigued polycrystalline nickel, a face-centered cubic (fcc) wavy slip metal, cyclically stressed from the virgin state to fracture using various specimens subjected to a variety of loading conditions. Although correspondingly detailed substructural evolution data are not available for 410Cb stainless steel, we consider those aspects of the evolutionary data for nickel that may be relevant to 410Cb stainless steel in its relation to the material nonlinearity parameter.

Martensitic 410Cb stainless steel has a body-centered tetragonal (bct) crystal structure and forms a lath-like morphology with a high dislocation density in the virgin state resulting from the large shear process in the displacive transformation from the body-centered (bcc) cubic austenite lattice. Martensitic alloys generally possess low stacking fault energies that favor planar dislocation slip[17]. However, the unusually high dislocation density of the alloy promotes a significant deformation by the formation of an increasingly finer dislocation cell structure that "would not be expected of planar dislocation formation unless dynamic strain aging of a low-temperature tempered structure occurs."[18] These opposing characteristics coupled with the paucity of data in the literature on the substructural evolution of 410Cb during fatigue leave to speculation the slip character of the alloy. In addition, 410Cb possesses precipitated secondary

phases that would be expected to complicate further the substructural evolution during the fatigue process.

Although the above considerations raise concerns over the applicability of the Cantrell model, based on substructrual evolution in wavy slip materials, to 410Cb stainless steel, the generic character of the model as embodied in Eq.(4) emphasizes that the more fundamental contribution to β is dependent on the dislocation monopoles and dipoles generated during the fatigue process. Further, the substructure data of Grobstein *et al.*[16] for polycrystalline nickel, obtained under a variety of widely disparate loading conditions, reveal that the volume fractions of veins and PSBs always increase monotonically during the fatigue process but with substantially different values that are dependent on the loading conditions. However, when using the data of Grobstein *et al.*[16] in Eq.(7), the calculated values of β all agree to within three percent after accounting for differences in the numbers of cycles to fracture[4].

The relative invariance of β to widely disparate loading conditions and values of substructural parameters, together with the generic linking of β via Eq.(4) to dislocation monopoles and dipoles, suggest that the manner in which the dislocation substructures evolve during fatigue may influence the value of β for a given fatigue state more than the specific values of the dislocation densities and volume fractions of the substructures involved. If this is so, then the model may be applicable to a wider variety of materials than previously thought by accounting appropriately for differences in the fundamental material parameters, such as the elastic moduli and Burgers vector, providing that the substructural evolution occurs in a manner that is organizationally and temporally (in terms of percent full life) similar to that of polycrystalline nickel.

Indeed, the substructures generated during the fatigue of metals do have somewhat similar evolutionary characteristics, whether the slip character of the material is wavy or planar slip[19]. The Luders bands (matrix structure) of planar slip materials are crudely analogous to the veins of wavy slip materials and increase in volume fraction in accordance with increasing fatigue loading cycles. The PSBs of wavy slip materials find a counterpart in the persistent Luders bands (PLBs) in planar slip materials that give rise to a strong generation of secondary dislocations as they mature. The PLBs do not represent zones of dislocation structure distinctly different from the matrix structure but are rather denser dislocation zones (bands) of activated primary slip planes. Thus, while the evolutionary substructures generated in planar slip materials are certainly different from that of wavy slip materials, the basic building blocks of the planar slip substructures are nonetheless dislocation monopoles and dipoles as in wavy slip materials. It is this common, yet tenuous, thread that we wish here to explore. Hence, it is with considerable trepidation and caution that the equations derived for wavy slip materials are applied here to martensitic 410Cb stainless steel with its uncertain slip character.

B. Calculation of model parameters for 410Cb stainless steel

We consider 410Cb stainless steel specimens cyclically loaded in stress-control at 551 MPa from zero to full load, a load corresponding to roughly 75 percent of the ultimate tensile strength of the material. Because of the uncertainty in the slip character of 410Cb, we use the terminology and dislocation substructure-related parameters obtained by Grobstein *et al.*[16] for wavy-slip polycrystalline nickel for cyclic loading in stress-control at 345 MPa, also a load corresponding to roughly 75 percent of the ultimate

tensile strength of the material. For such loads the vein structure attains a volume fraction $f_{vein} = 0.44$ at roughly10 percent full life and remains at that volume fraction to fracture. PSBs begin to form at approximately 0.1 percent full life and monotonically grow with decreasing slope to a volume fraction $f_{PSB} = 0.224$ at full life. The dislocation density in the PSB walls $\Lambda^{mp}_{PSBw} = 2.1 \times 10^{15}$ m^{-2}, the dislocation density in the vein structure $\Lambda^{mp}_{vein} = 1.05 \times 10^{15}$ m^{-2}, and the density of secondary dislocations generated as the PSBs mature is estimated from the work of Wang and Mughrabi[20] and Wang *et al.*[21] to be roughly 2.0×10^{15} m^{-2}. The dipole density in the vein structure $\Lambda^{dp}_{vein} = 5.25 \times 10^{14}$ m^{-2} and the dipole density in the wall structure $\Lambda^{dp}_{PSBw} = 1.05 \times 10^{15}$ m^{-2}. We assume[22,23] that the dipole height in the vein structure $h_{vein} = 7.6$ nm, the dipole height in the PSBs $h_{PSB} = 5.4$ nm, and the dislocation half-loop length $L = 8.2 \times 10^{-8}$ m. For 410Cb stainless steel[9,24] the shear modulus G = 68.6 GPa, the longitudinal modulus $A^e_2 = 277$ GPa, the Poisson ratio $\nu = 0.34$, and the magnitude of the Burgers vector b = 0.249 nm. For polycrystalline solids we assume $\Omega \approx R \approx 1/3$.

According to Mughrabi[25] the internal shear stress experienced by a given dislocation in the vein (matrix) structure is estimated to be roughly 20% of the saturation shear stress for the material. For engineering alloys the saturation stress is roughly equivalent to the endurance limit. The longitudinal stress endurance limit for 410Cb stainless steel[26] is approximately 410 MPa, corresponding to an endurance limit shear stress of roughly 205 MPa. Hence, the internal shear stress experienced by a given dislocation in the vein structure is approximately 41 MPa. The effective longitudinal stress $|\sigma_0|_{vein}$ in the vein structure is larger than the internal shear stress by the inverse Schmid factor R^{-1}. Thus, $|\sigma_0|_{vein} \approx 123$ MPa and the dislocation monopole contribution to

the nonlinearity parameter from the vein structure is calculated from Eq.(1) to be $\beta^{mp}_{vein} \approx 1342$. The gamma factor for dislocation monopoles in the vein structure is calculated from Eq.(5) to be $\Gamma^{mp}_{vein} = 2.11$.

A substantial contribution to the nonlinearity parameter is also obtained from the action of initial (internal) stresses on dislocations generated on secondary slip systems as the PSBs mature. From a consideration of Brown's model[14,27] for the internal stress fields of dislocation substructures we calculate from the analytical procedure reported by Cantrell[4] that the effective longitudinal stress $|\sigma_0|_{PSB\sigma}$ in the secondary dislocation structures of the PSBs is 75.9 MPa. Thus, the dislocation monopole contribution to the nonlinearity parameter from the mature PSBs is calculated from Eq.(1) to be $\beta^{mp}_{PSB\sigma} = 1576$. The gamma factor for dislocation monopoles associated with secondary dislocations is calculated from Eq.(5) to be $\Gamma^{mp}_{PSB\sigma} = 2.01$.

The calculation of the contribution to the nonlinearity parameter from dislocation dipoles in the vein structure is obtained by substituting the material constants and dislocation-related parameters given above into Eq.(2). We obtain $\beta^{dp}_{vein} = 38.7$ for the value of the dipole contribution associated with the vein structure. The gamma factor for dislocation dipoles in the vein structure is calculated from Eq.(6) to be $\Gamma^{dp}_{vein} = 0.11$. The dipole contribution to the nonlinearity parameter associated with the PSB wall (ladder) structure is obtained from Eq.(2) to be $\beta^{dp}_{PSBw} = 27.7$. The gamma factor for dislocation dipoles in the PSB wall structure is calculated from Eq.(6) to be $\Gamma^{dp}_{PSBw} = 0.11$.

The contribution to β from crack growth is calculated from Eqs.(8)-(10). For 410Cb stainless steel we assume[26] $n \approx 3.0$, $B = 1.13$ (penny-shaped cracks), and $K_{1c} \approx 60$

MPa√m. Experimental data is not available in the crack growth region for loading at 551 MPa. However, experimental data is available from measurements taken of 410Cb stainless steel steam generator turbine blades retired for cause because of cracking[28]. For these blades[29] the maximum cyclic stress is estimated to be roughly 70.3 MPa, $A \approx 3.1 \times 10^{-15} MPa^{-3} m^{-0.5} cycle^{-1}$, and $N_{total} \approx 2{,}3 \times 10^{11}$ cycles. We assume[6] that $C_{crk} \approx 10^{7}\ m^{-3}$.

Finally, the measured values of the effective Huang elastic constants $(A_2^e)_{effect}$ along the axis of cylindrical 410Cb specimens during fatigue shows a roughly one percent decrease from the value A_2^e measured in the virgin state[9]. From Eq.(12) such a decrease corresponds to an f_{WI} value of roughly 0.013 and indicates that relatively little of the damage region is interrogated by the ultrasonic weave. A decrease in $(A_2^e)_{effect}$ of a percent or two is common for measurements in the bulk of engineering alloys. For monocrystalline pure metals, decreases of ten percent have been reported[30].

C. Comparison of model to experimental data

The total nonlinearity parameters β for 410Cb stainless steel is plotted in Fig.1 as a function of percent fatigue life from the virgin state to fracture. The curve is calculated for stress-controlled cyclic loading at 551 MPa except for the portion of the curve in the Paris law regime, where the increase in β occurs by crack extension from pre-existing flaws at a loading stress of roughly 70.3 MPa. The experimental data points in the figure are taken from the work of Na *et al.*[9] and Kessel *et al.* [28] who obtained the β measurements from acoustic wave propagation along the axis of cylindrical samples taken from the gauge section of standard ASTM "dogbone" specimens. The measurements were taken on a series of specimens fatigued sequentially to a designated increased number of fatigue

cycles at 551 MPa and then prepared for acoustic harmonic generation measurements. The last two data points (in the crack propagation region) are taken on retired-for-cause steam generator blades for which percent life was estimated from inspection records.

It is important to note that significant variations (scatter) in the measured values of β occur in the 410Cb stainless steel experimental data, indicating that the fatigue damage is localized. The velocity measurements do not reveal a sufficiently large variation in the wave interaction factor f_{WI} to account for the measured variations in β. Such variations may result from variations in the internal stresses at the dislocation sites as the result of texturing, but a more likely cause is "premature" crack growth proximate to pre-existing flaws in the material. Indeed, the two data points in the Paris law region of Fig.1 show significant increases in β from cyclic loads (~70.3MPa) that are substantially below the endurance limit. Such growth can only result from crack growth initiated from preexisting flaws and substantiates the existence of pre-fatigue cracks or stress-raising flaws in the material. Variations in β may also result from large fluctuations in the dislocation densities in the material resulting from martensite formation. Indeed, the variations in β below roughly 0.1 percent fatigue life appear larger than the fluctuations above 0.1. This may indicate that the effects of density fluctuations are somewhat mollified as the result of the increased organization of the dislocations into substructures at increasing levels of fatigue.

Despite the scatter, there is generally quite good agreement between the experimental data and the theoretical curve. The agreement is surprisingly good when one considers that the theoretical curve is obtained by applying the substructural evolution data for polycrystalline nickel, a wavy slip fcc pure metal, to 410Cb stainless steel, a

martensitic alloy of uncertain slip character. Such agreement lends support to the notion that the analytical model may indeed be somewhat generic and thus applicable to a wide variety of metals. However, considerable caution must be exercised in such applications, since many of the microstructural input parameters used in the model calculations for both nickel and 410Cb stainless steel are based on educated estimates from other metals that are, as yet, experimentally unconfirmed for the present materials.

Notwithstanding such uncertainties, the present analytical model predicts and the experimental data generally show that the magnitude of the nonlinearity parameters of 410Cb stainless steel increase monotonically from the virgin state to fracture as the result of stress-controlled cyclic loading. It is significant that the nonlinearity parameter is a monotonically increasing function of the percent total fatigue life of the material, since a measured value of β then corresponds to a unique value of the total fatigue life. The contribution from substructural evolution accounts for an increase of almost 100 percent, despite the small value of the wave interaction factor f_{WI}. A measurable contribution from crack growth begins roughly at 95 percent of total fatigue life and rapidly becomes the dominant contribution to β as the crack increases in size to fracture. From Eq.(11) a larger value of f_{WI} would result in larger values of β, since the measurement volume would then contain a larger fraction of fatigue damage. However, such an increase does not diminish the fatigue-life predictive power of the measurement, since the values of β scale in exactly the same way over the whole range of percent total life. Indeed, the larger β scale would enable a more accurate assessment of the total fatigue life.

IV. CONCLUSION

The analytical model previously developed[1,4] of the nonlinear interaction of a stress perturbation (e.g., an acoustic wave) with organized dislocation substructures generated in wavy slip pure metals at a given state of fatigue is based on the accumulated nonlinearities of dislocation monopoles and dipoles that serve as building blocks for the substructures. The previous application[4] of the model to polycrystalline nickel and aluminum alloy 2024-T4 indicates that the manner in which the dislocation substructures evolve during fatigue may influence the value of β at a given fatigue state more than the specific values of the dislocation densities and volume fractions of the substructures involved. The dislocations substructures generated during fatigue of wavy slip materials have tenuous counterparts in planar slip materials that evolve in a somewhat similar temporal fashion to wavy slip substructures during the fatigue process. The similarity of the substructural evolution and the commonality of dislocation monopoles and dipoles as basic building blocks of the substructures, irrespective of slip character, provide a basis for applying the model, albeit cautiously, to a wider variety of metals than defined by the wavy slip origins of the model.

We have taken here the step of applying the model to 410Cb stainless steel. The agreement between the theoretical curve and experimental data in Fig.1 for 410Cb stainless steel is surprisingly good. Such agreement would not be possible, if appropriate accounting were not taken of the wave interaction volume. The wave interaction volume is quantified by the wave interaction fraction f_{WI} obtained from ultrasonic velocity measurements. Thus, it is important that careful velocity measurements be performed on

all materials to be evaluated for fatigue damage from nonlinearity parameter measurements.

The agreement between theory and experiment also suggests that the dislocation monopoles and dipoles do, indeed, dominate the substructural organization of 410Cb stainless steel and provide for a monotonic increase in the nonlinearity parameter during fatigue in a manner somewhat similar to that predicted for wavy slip metals. However, the details of the substructural organization, the temporal development of the substructures, the internal stresses developed in the substructures, the initially large dislocation densities and strains in the lath martensite structures, premature and arrested crack growth, crack tip plastic zones, and perhaps other as yet unknown factors, are most certainly responsible for contributions to the nonlinearity parameter not accounted in the model. Such contributions must be addressed in future studies. Indeed, a more comprehensive understanding of wave-microstructure interactions in a variety of metals and alloys and the assessment of model parameters resulting from such interactions at the most fundamental level must be acquired to gain confidence in model predictions and reliability. Such an understanding is presently being pursued through research with microscopically well-characterized single crystals and polycrystals of fatigued pure metals and metal alloys.

REFERENCES

1. J. H. Cantrell, Proc. R. Soc. London A **460**, 757 (2004).
2. J. H. Cantrell and K. Salama, International Materials Reviews **36**, 125 (1991).
3. W. T. Yost and J. H. Cantrell, Rev. Sci. Instrum. **63**, 4182 (1992).
4. J. H. Cantrell, Philos. Mag., in press.
5. P. C. Paris and F. Erdogan, Trans. ASME-J. Basic Engineering **85**, 528 (1963).
6. V. E. Nazarov and A. M. Sutin, J. Acoust. Soc. Am. **102**, 3349 (1997).
7. J. H. Cantrell and W. T. Yost, Philos. Mag. A **69**, 315 (1994).
8. J. H. Cantrell and W. T. Yost, International J. Fatigue **23**, S487 (2001).
9. J. K. Na, J. H. Cantrell, and W. T. Yost, in *Review of Progress in Quantitative Nondestructive Evaluation*, Vol. 15, eds. D. O. Thompson and D. E. Chimenti (Plenum, New York, 1996), p. 1347.
10. J. Frouin, S. Sathish, T. E. Matikas, and J. K. Na, 1999, J. Mat. Res. **14**, 1295 (1999).
11. P. Neumann,1983, in *Physical Metallurgy*, eds. R. W. Cahn and P. Haasen (Elsevier-Science, New York, 1983), p. 1554.
12. J. Kratochvil, Mater. Sci. Eng. **A 309-310**, 331 (2001).
13. D. Kuhlman-Wilsdorf and C. Laird, 1980, Mater. Sci. Eng, A **46**, 209 (1980).
14. L. M. Brown, in *Dislocation Modelling of Physical Systems*, eds. M. F. Ashby, R. Bullough, C. S. Hartley, and J. P. Hirth (Pergamon, Oxford, 1981), p. 510.
15. Z.-X. Tong and J.-P. Bailon, Fatigue Fract. Engng. Mater. Struct. **18**, 847 (1995).
16. T. L. Grobstein, S. Sivashankaran, G. Welsch, N. Paigrahi, J. D. McGervey, and J. W. Blue, Mat. Sci. Eng. A **138**, 191 (1991).

17. H.-J. Christ, in *ASM Handbook, Vol. 19, Fatigue and Fracture* (ASM International, Materials Park, OH, 1996), pp. 73.

18. G. Krauss, private communication.

19. C. Laird and L. Buchinger, Met. Trans. A **16A**, 2201 (1985).

20. R. Wang and H. Mughrabi, Mater. Sci, Eng. **63**, 147 (1984).

21. R. Wang, H. Mughrabi, S. McGovern, and M. Rapp, 1984, Mater. Sci. Eng. **63**, 219 (1984).

22. J. G. Antonopoulos and A. T. Winter, Philos. Mag. **33**, 87 (1976).

23. J. G. Antonopoulos, L. M. Brown, and A. T. Winter, Philos. Mag. **34**, 549 (1976).

24. R. W. K. Honeycombe, *Steels: Miocrostructure and Properties* (Edward Arnold, London, 1981)

25. H. Mughrabi, H., 1981, in *Proc. 4th Int. Conf. On Continuum Models of Discrete Systems*, eds. O. Brulin and R. K. T. Hsieh (North Holland, Amsterdam), p. 241.

26. S. Lampman, in *ASM Handbook, Vol. 19, Fatigue and Fracture* (ASM International, Materials Park, OH, 1996), pp. 712.

27. L. M. Brown, L. M. and S. L. Ogin, 1981, in *Dislocation Modelling of Physical Systems*, eds. M. F. Ashby, R. Bullough, C. S. Hartley, and J. P. Hirth (Pergamon, Oxford, 1981), p. 501.

28. G. L. Kessel, J. K. Na, W. T. Yost, and J. H. Cantrell, J. H.: "Nondestructive Inspection for Steam Turbine Blades," in *Proceedings of the ASME International Joint Power Generation Conference, New Orleans, LA, June 2001*.

29. H. Yu, “Phase I failure investigation for GE L-1 single boss blading,” Technical Report PA823, Stress Technology Incorporated, Rochester, NY.

30. H. M. Ledbetter, Phys. Status Solidi A **104**, 203 (1987).

FIGURE CAPTIONS

Fig. 1. Graph of material (acoustic) nonlinearity parameter plotted as a function of percent total fatigue life for martensitic 410Cb stainless steel fatigued in stress-controlled cyclic loading at 551 MPa. The continuous curve is calculated from the analytical model. The filled circles with error bars are experimental data points from Refs. 9 and 28 obtained from acoustic harmonic generation measurements.

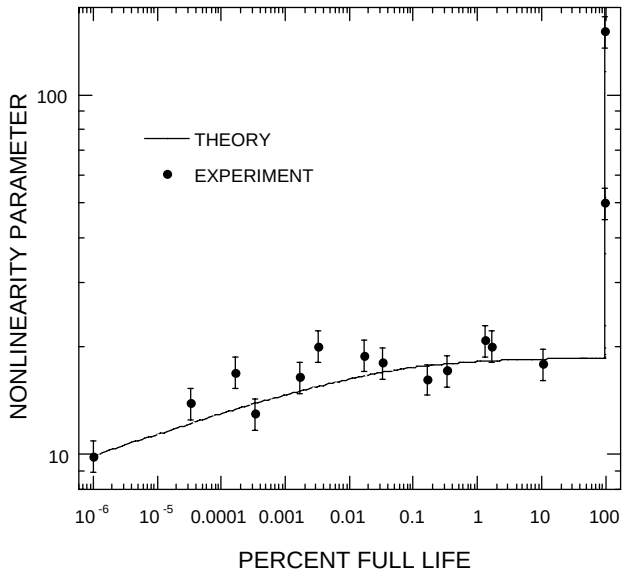

Fig. 1 Cantrell